HHS Public Access

Author manuscript

Mucosal Immunol. Author manuscript; available in PMC 2017 February 01.

Published in final edited form as:

Mucosal Immunol. 2017 January ; 10(1): 91–103. doi:10.1038/mi.2016.45.

Core 1- and core 3-derived *O*-glycans collectively maintain the colonic mucus barrier and protect against spontaneous colitis in mice

Kirk Bergstrom[1], **Jianxin Fu**[1,2], **Malin EV Johansson**[3], **Xiaowei Liu**[4], **Nan Gao**[5], **Qian Wu**[1,6], **Jianhua Song**[1], **J Michael McDaniel**[1], **Samuel McGee**[1], **Weichang Chen**[5], **Jonathan Braun**[7], **Gunnar C Hansson**[3], and **Lijun Xia**[1,2,8,*]

[1]Cardiovascular Biology Research Program, Oklahoma Medical Research Foundation, Oklahoma City, OK 73104, USA

[2]Jiangsu Institute of Hematology, Collaborative Innovation Center of Hematology, Key Laboratory of Thrombosis and Hemostasis of Ministry of Health, The First Affiliated Hospital of Soochow University, Suzhou, Jiangsu 215006, China

[3]Department of Medical Biochemistry, University of Gothenburg, 40530 Gothenburg, Sweden

[4]The Second Affiliated Hospital, Central South University, Changsha, Hunan 310051, China

[5]Department of Gastroenterology, The First Affiliated Hospital of Soochow University, Suzhou, Jiangsu 215006, China

[6]Department of Biochemistry and Molecular Biology, School of Basic Medical Sciences, Fudan University, Shanghai 200032, China

[7]Department of Pathology and Laboratory Medicine, David Geffen School of Medicine, University of California, Los Angeles, CA 90095, USA

[8]Department of Biochemistry and Molecular Biology, Oklahoma Center for Medical Glycobiology, University of Oklahoma Health Sciences Center, Oklahoma City, OK 73104, USA

Abstract

Core 1- and core 3-derived mucin-type *O*-glycans are primary components of the mucus layer in the colon. Reduced mucus thickness and impaired *O*-glycosylation are observed in human ulcerative colitis. However, how both types of *O*-glycans maintain mucus barrier function in the colon is unclear. We found that *C1galt1* expression, which synthesizes core 1 *O*-glycans, was detected throughout the colon, whereas *C3GnT*, which controls core 3 *O*-glycan formation, was

*Address correspondence to: Lijun Xia, M.D., Ph.D., Cardiovascular Biology Research Program, Oklahoma Medical Research Foundation, 825 N.E. 13th Street, Oklahoma City, OK 73104; Phone: 405-271-7892. Fax: 405-271-3137. Lijun-Xia@omrf.org.

AUTHOR CONTRIBUTIONS

K.B., J.F., M.E.V.J., G.C.H, L.X. designed the experiments; K.B., M.E.V.J. conducted the experiments; K.B., M.E.V.J., J.F., G.C.H, L.X. analyzed the data; X.L., N.G., J.S., J.M.M., S.M., provided technical help; W.C., J.B. critiqued the manuscript. K.B., J.F., L.X. wrote the manuscript.

DISCLOSURE

The authors declared no conflict of interest.

most highly expressed in the proximal colon. Consistent with this, mice lacking intestinal core 1-derived *O*-glycans (IEC *C1galt1*$^{-/-}$) developed spontaneous colitis primarily in the distal colon, whereas mice lacking both intestinal core 1- and core 3-derived *O*-glycans (DKO) developed spontaneous colitis in both distal and proximal colon. DKO mice showed an early onset and more severe colitis than IEC *C1galt1*$^{-/-}$ mice. Antibiotic treatment restored the mucus layer and attenuated colitis in DKO mice. Mucins from DKO mice were more susceptible to proteolysis than WT mucins. This study indicates that core 1- and 3-derived *O*-glycans collectively contribute to the mucus barrier by protecting it from bacterial protease degradation and suggests new therapeutic targets to promote mucus barrier function in colitis patients.

Keywords

mucin-type *O*-glycans; mucus layer; colitis; microbiota

INTRODUCTION

Ulcerative colitis (UC) is a major form of inflammatory bowel disease characterized by chronic inflammation of the colon.[1] The etiology of UC remains unclear, but mounting evidence suggests it is initiated and promoted by abnormal interactions of epithelial and immune cells with the intestinal microbiota in genetically susceptible individuals.[2] Defective barrier function of colon mucus has emerged as a significant factor contributing to UC pathogenesis.[3]

The colon is colonized by a dense, complex microbiota primarily composed of bacteria (10^{12}/ml).[4] These microbiota are normally sequestered from the mucosa by a mucus layer overlying the intestinal epithelium.[3,5] The structural basis of the mucus layer is a polymeric network primarily comprised of the MUC2 mucin, which forms an inner stratified layer attached to the mucosal wall that is bacteria-free, and a loosely-attached outer layer that is colonized by the microbiota.[6–8] MUC2 is extensively glycosylated with mucin-type *O*-linked oligosaccharides (*O*-glycans) that make up over 80% of its total mass.[9] In UC patients, reduced mucus thickness and impaired *O*-glycosylation are reported.[10,11] Muc2-deficient mice that lack a mucus layer develop spontaneous colitis,[8,12] indicating an important role of Muc2 in mucus function and homeostasis.

O-glycans on Muc2 are of the core 1- and core 3-derived type,[13] which are built on the initial structure (GalNAcα-*O*-Ser/Thr, also called Tn antigen) within proline/serine/threonine-rich domains of the mucin protein core.[14] The core 1 β1,3-galactosyltransferase (C1GalT1), which is ubiquitously expressed, is solely responsible for the synthesis of core 1 *O*-glycans.[15] In contrast, core 3 β1,3-N-acetylglucosaminyltransferase (C3GnT), which controls the biosynthesis of core 3 *O*-glycans, is expressed mainly in the intestine and salivary glands.[13] Both types of structures can be further extended and/or branched to form sialylated and/or sulfated core 1- or 3-derived *O*-glycans such as core 2 or 4 O-glycans.[16,17] Our previous studies show that mice lacking C3GnT (*C3GnT*$^{-/-}$) are more susceptible to chemically-induced colitis,[13] and intestinal epithelial-specific deletion of C1GalT1 (IEC *C1galt1*$^{-/-}$) leads to spontaneous colitis.[11] Yet, whether core 1 and core 3 *O*-glycans

differentially contribute to mucin barrier function and how *O*-glycans preserve mucus integrity remain unclear.

To address these questions, we generated a new mouse model that lacks both intestinal core 1- and core 3-derived *O*-glycans (DKO). We found that core 3-derived *O*-glycans play an important role in the protective functions of mucus in the proximal colon where they are more highly expressed, and both types of *O*-glycans are required for colitis protection in the distal colon. Our results show that Muc2 requires both types of *O*-glycans to protect it from degradation by microbiota-derived proteolytic factors.

RESULTS

Core 1- and 3-derived *O*-glycans collectively contribute to mucus barrier function and colitis protection in the distal colon

To address whether core 1- and core 3-derived *O*-glycans collectively contribute to mucus barrier integrity and colitis protection, we generated a new mouse line lacking intestinal core 1- and core 3-derived *O*-glycans (DKO) by crossing IEC *C1galt1*$^{-/-}$ mice with *C3GnT*$^{+/-}$ mice (Supplementary Figure 1a). We compared colitis development of *C3GnT*$^{-/-}$, IEC *C1galt1*$^{-/-}$ and DKO mice with wild-type (WT) littermates.

Consistent with our published studies, *C3GnT*$^{-/-}$ mice exhibited no colitis phenotype without challenge, and IEC *C1galt1*$^{-/-}$ mice developed spontaneous colitis by 2 weeks of age.[10,13] DKO mice started to develop spontaneous colon inflammation as early as postnatal day 8 (P8) (Figure 1b and Supplementary Figure 1b), which progressed rapidly (Figure 1a and b). To determine if a greater defect in the distal colonic mucus layer contributes to the earlier disease onset in DKO mice, we analyzed mucus layer structure in P7 WT and mutant mice, prior to colitis (Figure 1b and Supplementary Figure 1c). Alcian blue (AB) staining of Carnoy's-fixed colonic sections revealed a clear inner stratified mucus layer in WT mice at P7, which was similar in *C3GnT*$^{-/-}$ mice and even IEC *C1galt1*$^{-/-}$ mice at this age; in contrast, the inner mucus layer thickness was significantly reduced in DKO mice (Figure 1c and d). Immunohistochemistry (IHC) for Tn-antigen, exposed when lacking both core 1 and core 3 *O*-glycans, confirmed the presence of truncated *O*-glycans in goblet cells and the inner mucus layer of IEC *C1galt1*$^{-/-}$ and DKO littermates (Figure 1e and f).

To investigate whether the impaired mucus layer impacted tissue-microbiota interactions, we performed dual staining for the major colonic mucin Muc2, and luminal bacteria via fluorescence in situ hybridization (FISH) with the universal bacterial probe EUB338. A progressive reduction of the mucus barrier between the microbiota and the mucosal surface was observed in DKO mice vs. all other groups (Supplementary Figure 1d). At P12 bacteria were in direct contact with the mucosa in the DKO colon (Figure 1g). An intestinal permeability assay using fluorescein isothiocyanatedextran (FITC-dextran, FD4, 4 kDa) revealed a significant increase in barrier permeability in both IEC *C1galt1*$^{-/-}$ and DKO mice relative to WT mice (Figure 1h). By P21, the mucus layer was absent in DKO mice, and dramatically reduced in IEC *C1galt1*$^{-/-}$ mice compared to WT and *C3GnT*$^{-/-}$ mice (Figure 1d). At this time point, colitis was most severe in DKO mice, evidenced by histologic scoring, elevated proinflammatory cytokine expression, and polymorphonuclear cell

infiltration (Figure 1b, Supplementary Figure 1e, f). Collectively, these results indicate that the degree of intestinal *O*-glycan loss is directly correlated with the level of mucus layer impairment as well as colitis onset and severity.

Loss of both core 1- and core 3-derived *O*-glycans affects mucus layer structure and colitis susceptibility throughout the colon

Although core 1 *O*-glycosylation is most important for mucus barrier function in the distal colon, whether this is the case in the proximal colon was unclear. To address this, we compared disease and *O*-glycosylation status in the proximal colon of WT and IEC *C1galt1*$^{-/-}$ mice. Relative to the distal colon, *O*-glycosylation was intact in goblet cells, a mucus layer was visible, and colitis was minimal in the proximal colon of 3 month-old IEC *C1galt1*$^{-/-}$ mice vs. WT littermates based on AB staining (Supplementary Figure 2a – d). We therefore hypothesized that core 3-derived *O*-glycans protect IEC *C1galt1*$^{-/-}$ proximal colon from spontaneous disease. Gene expression analysis of enriched colon crypt cells by RT-qPCR showed higher levels of *C3GnT* expression in the proximal colon of WT and IEC *C1galt1*$^{-/-}$ mice than that of the distal colon (Figure 2a), consistent with AB staining (Supplementary Figure 2); in contrast, *C1galt1* was expressed at similar levels in the proximal and distal colon of WT mice, but not of IEC *C1galt1*$^{-/-}$ mice as expected (Figure 2a). These results show a differential expression pattern of *C3GnT* in different regions of the murine colon.

To show that both core 1- and 3-derived *O*-glycans contribute to mucus layer integrity in the proximal colon, we compared glycosylation, mucus layer, and disease status of this region between 3 month-old WT, *C3GnT*$^{-/-}$, IEC *C1galt1*$^{-/-}$ and DKO mice. IHC for Tn antigen revealed that the percent of Tn-positive (Tn^{+}) proximal goblet cells was 100% in DKO mice, compared to ~50% Tn^{+} in IEC *C1galt1*$^{-/-}$ mice, and no Tn^{+} goblet cells in WT and *C3GnT*$^{-/-}$ mice (Figure 2b). In contrast, distal colonic Tn expression was comparable between IEC *C1galt1*$^{-/-}$ and DKO mice at this age (Supplementary Figure 3). To examine the relationship between Tn expression patterns and proximal colon mucus layer integrity, we immunostained Carnoy's-fixed colon tissues (with stool intact) of each strain for Muc2 and compared inner mucus layer structure. WT and *C3GnT*$^{-/-}$ mice showed a Muc2-rich inner mucus layer separating luminal content from the mucosa; IEC *C1galt1*$^{-/-}$ mice had reduced thickness of the inner mucus layer and DKO mice had a complete loss of the layer (Figure 2c and d). To determine if this impacted colitis susceptibility, we analyzed H&E-stained colon sections. Spontaneous inflammation in proximal colon regions was observed in DKO but not WT, *C3GnT*$^{-/-}$, and IEC *C1galt1*$^{-/-}$ mice (Figure 2e and f). Thus, whereas colitis protection in the distal colon is primarily dependent on core 1 *O*-glycans, both core 1- and 3-derived *O*-glycans cooperate in the proximal colon to preserve mucus barrier integrity.

Both core 1- and 3-derived *O*-glycans contribute to mucus layer establishment and colitis protection in adult mice

Our data show that constitutive loss of *O*-glycans during embryonic and postnatal development affects mucus layer structure and colitis severity, but it was not clear whether loss of intestinal *O*-glycans during adulthood would have similar consequences. To address this question, previously described mice with tamoxifen (TM)-inducible deficiency of

C1GalT1 (TM-IEC *C1galt1*$^{-/-}$)[10] on a C3GnT$^{+/-}$ background were bred with *C3GnT*$^{+/-}$ mice to generate WT, TM-IEC *C1galt1*$^{-/-}$ and TM-DKO littermates (Figure 3a). We treated 10 – 12 week-old littermate WT, TM-IEC *C1galt1*$^{-/-}$, and TM-DKO with TM for 5 consecutive days, and sacrificed all mice 5 and 10 days after final TM treatment for mucus and disease analysis (Figure 3b). By histology, colitis occurred in both TM-IEC *C1galt1*$^{-/-}$ and TM-DKO mice, although it was most severe in TM-DKO mice at 5 and especially 10 days post-TM (Figure 3c and d). To determine the relationship of colitis onset to the mucus layer, we performed AB staining. A loss of AB-stained mucus layer was obvious in the distal colon of TM-DKO mice by 5 days, compared to WT and TM-IEC *C1galt1*$^{-/-}$ littermates, the latter still showing a thin mucus layer even at 10 days post TM (Figure 3d and e). Immunofluorescent staining (IF) for Muc2 and Tn-antigen revealed that most goblet cells in the distal colon of both strains expressed mucin with truncated *O*-glycans (i.e. dually Muc2^{+}Tn^{+}) (Figure 3e and f). However, some TM-IEC *C1galt1*$^{-/-}$ mice at 5 days post TM, and to a lesser extent at 10 days post TM, showed a mixed Tn^{+} and Tn-negative (Tn^{-}) inner mucus layer, with the truncated *O*-glycan (i.e. Tn^{+}) portion being contributed directly by mucosal goblet cells (Figure 3e), suggesting core 3 *O*-glycans on the luminal side were somehow protecting its loss. In the proximal colon, AB staining intensity was lower in TM-DKO vs. TM-IEC *C1galt1*$^{-/-}$ mice (Supplementary Figure 4a). Dual Muc2/Tn staining revealed a greater fraction of proximal colonic goblet cells were expressing truncated *O*-glycans on mucin (i.e. Muc2^{+}Tn^{+}) in TM-DKO mice vs. TM-IEC *C1galt1*$^{-/-}$ mice, while all proximal goblet cells in WT mice harbored normal mucin (i.e. Tn^{-}) in their secretory granules (Supplementary Figure 4c and d). Consistent with this, the proximal colon mucus layer of TM-IEC *C1galt1*$^{-/-}$ mice showed mixed Tn expression, whereas this layer was gone in TM-DKO mice (Supplementary Figure 4b and c). These results indicate core 3-derived *O*-glycans contribute to mucus layer integrity and affect colitis development after induced deletion of core 1 *O*-glycans in adult mice.

Antibiotic treatment improves mucus layer and reduces severity of colitis in DKO mice

To address whether an inner mucus defect leads to increased bacterial interactions with the epithelium and subsequently contributes to colitis, WT and DKO mice were treated with broad-spectrum antibiotics (neomycin sulfate, metronidazole, vancomycin, ampicillin; NMVA) for 4 weeks (Figure 4a),[10,18] followed by mucus layer structure and disease analysis. As expected, NMVA significantly reduced bacterial levels in NMVA- vs. vehicle-treated mice, as tested by qPCR of bacterial 16S rRNA for total bacteria, and for bacterial subsets belonging to different phyla (Figure 4b). Dual Muc2 IF/EUB338 FISH analysis revealed that, in vehicle-treated groups, bacteria were in direct contact with the mucosa in DKO mice, which lacked a mucus layer, whereas bacteria were separated from epithelia by an inner mucus layer in WT mice (Figure 4c). In the NMVA-treated groups, EUB338 signal was not detected, and a thick inner layer mucus was maintained in WT mice; in contrast, a thin mucus layer was observed in DKO mice (Figure 4c). To determine whether the improved mucus layer in treated DKO mice resulted from the presence of intact mucins, we extracted colon luminal mucus scrapes and analyzed them via composite agarose-polyacrylamide gel electrophoresis (AgPAGE)[19] followed by in-gel periodic acid/Schiff (PAS staining), which stains neutral as well as acidic mucins. Vehicle-treated WT mice had a strong 1 – 2 MDa band but only a faint band was detected in vehicle-treated DKO mice. In

contrast, a high molecular weight (MW) band was evident in NMVA-treated DKO secretions, migrating between the two major bands in WT mice (Figure 4d).

We next investigated how loss of *O*-glycans impaired mucin stability. Although mucus Muc2 is primarily modified by *O*-glycans, N-glycans are present in the C-terminal cysteine-knot of human and rodent Muc2. Fucose (Fuc) is a common capping structure on both *O*- and N-glycans. In DKO mice, *O*-glycans are truncated to Tn antigen and thus do not carry any fucose (Fuc), however, Fuc on N-glycans of Muc2 should not be affected.[20] Therefore, Fuc can be used as a marker for monitoring the stability of Muc2. We used the lectin *Ulex europaeus* agglutinin-1 (UEA1, binds Fucα1,2Gal epitopes) to stain the tissue and found that luminal UEA1 was detected in WT mucus as expected (Figure 4e). NMVA-treated WT showed a slightly increased UEA1 staining, suggesting some Fuc on *O*- or N-glycans are susceptible to bacteria-mediated degradation. In contrast, no luminal UEA1 was seen in the DKO tissue, however, similar to Muc2 staining, a thin UEA1-rich layer was observed overlying the mucosal surface of NMVA-treated DKO mice (Figure 4e). These results support that bacteria-derived enzymes digest *O*-glycan-deficient mucins even in the presence of N-glycans as monitored by Fuc labeling. Notably, colitis severity was dramatically reduced in NMVA-treated DKO mice (Figure 4f). Collectively, these studies indicate that the *O*-glycans are critical for mucin stability and a partial rescue of the mucus layer in DKO mice is associated with amelioration of inflammation, and suggest colitis is driven by bacterial-mucosal interactions following mucus barrier breach.

Loss of the mucus barrier in DKO mice is dependent upon the microbiota but not inflammation

Both inflammation and microbiota may affect mucus structure and glycosylation.[11,19] To determine whether loss of the mucus layer in DKO mice is caused by bacterial factors prior to inflammation, we orally administered a high-dose (20 mg) of the aminoglycoside antibiotic streptomycin (strep) to WT and DKO mice once a day for 2 days, then analyzed these mice for mucus integrity (Figure 5a). This antibiotic was chosen due to its rapid action[21,22] and broad-spectrum activity at high doses against many Gram-negative and Gram-positive facultative anaerobes[23] as well as obligate anaerobes such as *Bacteroides*[24]. Indeed, qPCR analysis of fecal content revealed that this treatment led to an approximately a 1000-fold drop in total microbiota (Figure 5b), and a 10,000 fold decrease in the Bacteroidales order, in DKO mice (Figure 5c). The overall reduction in total microbiota was confirmed independently by FISH analysis of colonic cross sections (Figure 5d). Importantly, the severity of colitis between strep-treated and non-treated mice was no different due to the short time frame of antibiotic treatment (Figure 5e). However, strep-treated DKO mice exhibited a clear and obvious Tn^+ mucus layer, while no visible mucus layer was found overlying the surface on untreated DKO mucosa (Figure 5f). To investigate whether strep-treatment rescues Muc2/mucus quantitatively, we extracted mucus secretions of untreated or strep-treated WT and DKO mice, separated them via AgPAGE, and visualized them by PAS staining. Consistent with the Muc2 staining on colonic cross sections, we found a more intensely PAS-stained high molecular weight band in strep-treated DKO mice vs. untreated mice (Figure 5g).

O-glycans protect Muc2 from bacterial protease-mediated degradation

The above results suggest that the loss of mucus layer integrity in *O*-glycan-deficient mice is largely dependent on the microbiota but independent of inflammation. Indeed, bacteria could be seen between a broken, discontinuous mucus layer remaining in some DKO mice, in contrast to a continuous mucus layer in NMVA-treated DKO mice (Figure 6a). Although bacterial glycosidases, sulfatases, and proteases may contribute to mucus layer breakdown,[19,25,26] we hypothesized that proteases play a major role. We tested this directly by treating mucus extracted from strep-treated WT and DKO mice with or without pronase, a mixture of proteases derived from *Streptococcus sp.*, (1 mU for 30 min). Subsequent analysis by AgPAGE and PAS staining revealed a minimal effect of pronase on WT mucus, demonstrated by a modest downward shift of the high MW band. In contrast, pronase treatment led to a dramatic loss of the high MW PAS-stained band compared to non-treated DKO mucus (Figure 6b).

To confirm this effect on the Muc2 mucin, we repeated the assay on isolated WT and DKO mucin treated with increasing doses of pronase, followed by western blotting using the UEA1 lectin to analyze mature (glycosylated) Muc2, and an anti-Muc2-C3 antibody (against Muc2 C-terminus) that recognizes total (glycosylated and unglycosylated) Muc2.[8] This approach was necessary because the Muc2-C3 antibody has greater affinity toward less glycosylated mucin (Supplementary Figure 5a, b and d), whereas UEA1 readily binds mature mucin from WT and DKO mice (Supplementary Figure 5c and d). Of note, mucosal extractions also included a ~ 500 kDa non-glycosylated Muc2 band (i.e negative for PAS, UEA1 and Tn-antigen) (Supplementary Figure 5b–d), likely the intracellular Muc2 apomucin from sloughed epithelial cells found in secretions, or deglycosylated by bacteria.

Pronase treatment revealed mature ($UEA1^+$) WT Muc2 remained intact even at the highest dose of 1 mU, while the $UEA1^+$ $Muc2^+$ band from DKO mucin began being degraded at the lowest dose (0.01 mU) and was completely gone at the 1 mU dose, consistent with the PAS staining (Figure 6c). Importantly, the non-glycosylated Muc2 band was degraded in both WT and DKO samples (Figure 6c), providing an internal control for protease activity and proof-of-principle that core 1- and 3-derived *O*-glycans afford protection against proteolysis. In addition, this non-glycosylated Muc2 protein showed a faster rate of degradation in DKO vs. WT mucin preparations in response to increasing levels of pronase, suggesting the glycosylation status of the mature mucin could provide protection for the unglycosylated mucin against proteolytic attack (Figure 6c). Densitometry indicated DKO Muc2 was between 10 – 100-fold more susceptible to degradation by pronase than WT Muc2 (Figure 6d).

Taken together, these results reveal that loss of mucin-type *O*-glycans renders Muc2 more susceptible to bacterial-derived proteolytic degradation, which in turn protects the mucosa from bacteria-induced inflammation.

DISCUSSION

The mucus layer plays a key barrier role in the colon where the resident microbiota exists at the highest density and diversity relative to other regions of the intestine.[27] *O*-glycans are the

major components of the polymeric Muc2 mucin that forms this mucus layer. Our study reveals that the two major types of *O*-glycans, core 1- and core 3-derived, are differentially expressed in the colon, and collectively contribute to mucus layer integrity and prevent microbiota-driven colitis. Mechanistically, core 1- and 3-derived *O*-glycans promote mucin stability in the presence of bacterial-derived proteases. This critical function preserves mucus barrier integrity and prevents the unrestricted access of the microbiota to the mucosa that would otherwise lead to spontaneous chronic inflammation.

We found that C3GnT expression was higher in the proximal than in the distal colon, in contrast to C1GalT1 expression that was highly expressed throughout the colon. This new finding explains why the colitis phenotype is mainly limited to the distal colon of IEC *C1galt1*$^{-/-}$ mice, while colitis occurs throughout the colon in DKO mice. Interestingly, colitis in proximal colonic regions of DKO mice was less severe than in the distal colon. It is possible that this phenotype may be linked to region-specific microbiota communities as differences in abundance and diversity of the mucosa-associated microbiota in the proximal vs. distal regions have been reported, Regardless, our results underscore the essential role of *O*-glycosylation in general in regulating homeostasis of the colonic mucus layer.

Our data show that the degree of *O*-glycosylation directly impacts the ability to maintain a functional mucus layer in the presence of the microbiota in the colon. How do *O*-glycans preserve mucus integrity? Glycosidase activity is an inherent aspect of the microbiota, which plays key roles in maintenance of some community members who ferment it for energy and catabolize it to modulate their cell walls[30–32]. We observed rescue of N-glycosylated mucus after antibiotic treatment, suggesting that bacteria-derived glycosidases may break down or inhibit further modifications of the residual GalNAc structures on mucins from the DKO colon. Muc2 of the DKO colon still has the GalNAc structure. However, our data show that this residual structure is not sufficient to protect Muc2 from degradation in the colon where microbiota-derived glycosidases and proteases readily break down the core 1- and core 3-deficient Muc2. This is of relevance in human UC, where, in addition to *O*-glycan defects, increased overall mucolytic activity of fecal contents was observed compared to healthy controls,[25] therefore likely rendering UC mucus more unstable and susceptible to breach.

Although our findings support that *O*-glycans function primarily to promote Muc2 stability, it is possible that *O*-glycosylation also influences establishment of a stable mucus layer. For example, mucin-type *O*-glycosylation has been linked to promoting optimal secretion of proteins that protect the digestive tract of *Drosphila* larvae.[33] In our study, we observed a relatively intact mucus layer in neonatal DKO pups (P7) or in adult DKO mice with greatly diminished bacteria after antibiotic treatment, supporting that mucin secretion is not significantly impaired in the absence of both types of *O*-glycans. Nevertheless, as the mucus layer is constantly renewed and degraded, further studies are needed to determine any possible role of *O*-glycosylation in regulating the maturation and trafficking of Muc2 and/or other mucus-associated proteins to promote the homeostasis of the mucus layer.

Recent studies have shown *O*-glycans influence microbiota composition; for example, induced loss of C1GalT1 alters microbial communities in the distal colon.[34,35] Similar findings were reported with mice deficient in fucosyltransferase 2 (Fut2) responsible for

terminal fucosylaton of glycans, and the galactosyltransferase β4GalnT2 that forms the terminal Cad carbohydrate antigen.[36,37] The basis for this selection and whether glycan-mediated influences on microbiota composition reflect a dysbiotic community that potentiates colitis is unclear, although Fut2-deficiency has recently been linked to Crohn's disease.[37,38] However, it is notable among genetic studies with targeted deletion of glycosyltransferases, to our knowledge, only lack of C1GalT1 has been shown to overtly impact mucus layer structure and elicit spontaneous colitis. This suggests a preeminent role of mucus barrier function vs. other functions in promoting homeostatic interactions with intestinal microbiota. However, it remains to be addressed whether unique bacterial species, perhaps influenced by *O*-glycosylation, are required for mucus breakdown and/or colitis development.

Although all mucins, including membrane bound and secreted forms, require core 1 and 3 *O*-glycosylation, the Muc2 mucin appears to be the most critical. Several mucin-deficient mouse lines have been reported (e.g. Muc1, Muc13), but only deletion of Muc2 results in spontaneous disease similar to DKO mice.[12,39] The dynamics of disease progression differ between DKO and *Muc2*$^{-/-}$ mice: colitis is evident between 1 – 2 weeks in DKO (on a C57BL/6J or mixed B6/129Sv background) mice, but only by 8 weeks in *Muc2*$^{-/-}$ mice on a B6 background.[39] This difference may be due to the fact that loss of core 1 and 3 *O*-glycans in DKO causes defects in many mucins including Muc2. Indeed, membrane-bound mucins such as Muc1 and Muc13 have been shown to be important for intestinal barrier function during pathogen infection.[40,41] However, environmental influences (e.g. facility-dependent microbial communities) may also readily explain the differences in Muc2 and intestinal *O*-glycan-deficient mice, since disease dynamics in *Muc2*$^{-/-}$ and DKO mice from the same facility have not yet been compared side by side. Regardless, our findings add crucial insights into how the colonic mucus layer is maintained when Muc2 expression is intact, namely through core 1- and 3-derived *O*-glycan-mediated Muc2 stabilization in the colon.

The innate immune system directly responds to microbial-derived signals through pattern recognition receptors such as Toll-like receptors (TLRs) and Nod-like receptors (NLRs), although their roles in microbiota-induced disease appears contingent upon the genetic defect predisposing to colitis. For example, spontaneous colitis in *Il10*$^{-/-}$ mice[42] or IEC *IKKγ*$^{-/-}$ [43] mice is dependent on TLR signaling by the microbiota. Conversely, spontaneous colitis in *Il2*$^{-/-}$ mice is completely independent of TLR signaling,[42] and deficiency of some TLRs (TLR5) can itself predispose to spontaneous colitis.[44] Interestingly, our previous report shows that the initiation of spontaneous colitis in IEC *C1galt1*$^{-/-}$ mice was independent of most TLR-dependent signaling, including TLR4.[10] In a separate study, we recently found spontaneous colitis in DKO mice was controlled by caspase 1-dependent inflammasomes (Bergstrom et al, unpublished). Since DKO mice exhibit UC-like colitis, delineating the innate pathways that drive disease will provide insights into how mucus layer regulates homeostasis with the resident microbiota.

Collectively, these findings provide insights into the regulation of colon homeostasis by mucin-type *O*-glycans, and lend key insights into the basis and pathogenic potential of similar mucus defects observed in UC. By promoting the formation of a stable mucus network overlying the epithelium, core 1- and 3-derived *O*-glycans preserve a mutualistic

interaction with resident microbiota that keeps immune responses below their threshold of activation. In addition, compared with other colitis mouse models, the DKO develop reproducible colitis on either C57BL/6J or mixed B6/129Sv. Therefore, it provides not only a more clinically relevant opportunity to dissect how components of the microbiota or the immune system contribute to each stage of colitis pathogenesis, but also a valuable model to test pharmacological interventions.

METHODS

Mouse breeding

WT and IEC *C1galt1*$^{-/-}$ were generated by mating *C1galt1*-floxed (*C1galt1*$^{f/f}$) mice with VillinCre transgenic mice as described.[10] To produce dual intestinal core 1- and core 3 *O*-glycan-deficient (DKO) mice, *C1galt1*$^{f/f}$;*C3GnT*$^{+/-}$ females were crossed with *C3GnT*$^{+/-}$;*C1galt1*$^{f/f}$;VillinCre^{+} males to generate *C3GnT*$^{-/-}$, IEC *C1galt1*$^{-/-}$, DKO, and WT littermates. To induce a postnatal deficiency of *O*-glycans, *C3GnT*$^{+/-}$;*C1galt1*$^{f/f}$ mice were first crossed with previously generated *C1galt1*$^{f/f}$;VillinCre-ER^{T2} (TM-IEC *C1galt1*$^{f/f}$) mice[10] on a *C3GnT*$^{+/-}$ background to generate TM-IEC *C1galt1*$^{f/f}$;VillinCre-ER^{T2}, TM-IEC *C1galt1*$^{f/f}$;*C3GnT*$^{-/-}$;VillinCre-ER^{T2}, and WT (TM-IEC *C1galt1*$^{f/f}$) littermates. To generate TM-IEC *C1galt1*$^{-/-}$ and TM IEC *C1galt1*$^{-/-}$;*C3GnT*$^{-/-}$ (TM-DKO) mice, 10- to 12-week-old mice were injected intraperitoneally with 1 mg tamoxifen (TM) (MP Bio-medicals) in an ethanol/sunflower seed oil mixture (1:9 [v/v]) for 5 consecutive days. All mice are on a C57BL/6J and 129/SvImJ mixed background, except for the TM-inducible lines, which are on a B6 congenic background. Animals were fed standard chow (PicoLab Rodent Diet 20). All animal studies were carried out in a specific pathogen free (SPF) environment according to animal welfare regulations stipulated by IACUC.

Tissue preservation and histology

For histology, tissues were freshly harvested from mice and fixed with 10% neutral buffered formalin or in Carnoy's fixative (60% methanol, 30% chloroform, and 10% acetic acid) prior to paraffin embedding. Paraffin-embedded sections (5 μm) were stained with H&E. The pictures were obtained with a Nikon Eclipse E600 microscope equipped with a Nikon DS-2Mv camera, using the software NIS Freeware 2.10. Histologic severity of colitis was determined as described below.

Histologic scoring

Histologic scoring was performed using a modified protocol from Haezelwoood et al (2008). The following parameters and their respective scoring is as follows polymorphonuclear (PMN) cell infiltration per high-power field (HPF; 40×) (0 to 5 = 0; 6 to 10 = 1; 10 to 20 = 2; >20 = 3); Mononuclear cell infiltration per HPF (None (<1× WT) = 0; Mild (1 to 2× WT) = 1; Moderate (2 to 3× WT) = 2; Severe (>3× WT) = 3); Mucosal hyperplasia (<1× thickness of WT = 0; 1 to 1.5× thickness of WT = 1; 1.6 to 2× WT = 2; >2× WT = 3); Goblet cell loss (<10% loss vs. WT = 0; 11 – 25% loss vs. WT = 1; 25 to 50% loss vs. WT = 2; >50% loss vs. WT = 3); crypt abscesses (# per section: 0 = 0, 1 to 5 = 1, 6 to 10 = 2, >10 = 3). The highest score to be obtained is 15. Scoring was performed under blinded conditions by an independent observer. For PMN and mononuclear cell infiltration, and

goblet cell enumeration, the mean value over 4 – 5 HPFs was determined and used for the final value. For mucosal thickness assessment, the mean value for each section was taken from 8 – 10 digital measurements over regular intervals of the length between the muscularis mucosa and the surface epithelium.

Histological staining of mucins

Carnoy's fixed sections were cut (5 μm), deparaffinized and hydrated using standard protocols. Sections were then immersed with Alcian blue (AB) pH 2.5 (Newcomer Supply), which stains acidic mucins a light blue,[10] for 20 min and then thoroughly rinsed in tap water. Sections were counterstained with nuclear fast red for 10 min, dehydrated and mounted with Permount and imaged.

Immunostaining

Formalin-or Carnoy's-fixed paraffin-embedded sections were deparaffinized and rehydrated. For Streptavidin-biotin-based staining, sections were first blocked with Streptavidin/Biotin Blocking Solution (Vector Labs). For immunohistochemistry (IHC), endogeneous peroxidase blocking was performed by incubation with 3% H_2O_2 for 10 min at room temperature (RT). For Immunoepifluorescence (IF) or IHC, Serum-Free Protein Block (DAKO) was used to block non-specific antibody binding (10 min, RT). Following blocking, sections were incubated with rabbit anti-MUC2 (H300 Santa-Cruz), and/or biotinlyated mouse anti Tn-antigen IgM (provided by Tongzhong Ju and Richard Cummings, Emory University, Atlanta, Georgia, USA), or rabbit anti murine MPO (5 μg/ml, clone 1A8; BD), overnight at 4°C. For anti-MPO detection, sections were stained with Cy-3 labeled goat anti–rabbit IgG (1:50; Jackson ImmunoResearch Laboratories Inc.). For MUC2 immunofluorescent staining, sections were incubated with biotinylated goat anti-rabbit IgG (1.5 μg/ml) and then with DyLight 488-labeled Streptavidin (ThermoScientific) (5 μg/ml) for 30 min at RT. For dual Muc2-Tn epifluorescence, sections were incubated with Cy-3-labeled goat anti–rabbit IgG and DyLight 488-labeled Streptavidin. Sections were then counterstained with 25 ng/ml DAPI in dH_2O for 3 min, then washed with dH_2O and mounted using PermaFluorAntifade (ThermoScientific). For anti Tn-antigen IHC, sections were incubated with HRP-conjugated Streptavidin (2 μg/ml; Jackson immunoresearch) for 40 min at RT and detected using the DAB staining kit (Vector), and counterstained with hematoxylin, dehydrated and mounted. For epifluorescent imaging, specimens were analyzed with a Nikon Eclipse 80*i* microscope equipped with a Nikon DS-Qi1MC camera operating through NIS Elements AR software (v3.0). For imaging IHC staining, sections were imaged by brightfield as above. Species-specific, isotype control antibodies or non-primary antibody-treated sections were used for negative controls.

FISH and dual Muc2/FISH labeling

For fluorescence in-situ hybridization (FISH), stool pellet containing-colon sections fixed with Carnoy's fixative were incubated with Texas red–conjugated universal bacterial probe EUB338 (5′-GCTGCCTCCCGTAGGAGT-3′; bp 337–354 in bacteria EU622773), or with a nonspecific probe (NON338 5'-ACTCCTACGGGAGGCAGC-3') as a negative control, (both from MWG/Operon) in hybridization buffer (20 mM Tris-HCl, pH 7.4; 0.9 M NaCl; 0.1% SDS) at 37°C overnight. The sections were rinsed in wash buffer (20 mM Tris-HCl,

pH 7.4; 0.9 M NaCl) 37°C for 15 min. For dual Muc2-FISH labeling, sections were stained with Muc2 as above prior to FISH.

Calculation of mucus thickness

For determination of mucus thickness using Alcian-blue or Muc2-stained tissue sections, 15 – 30 measurements were taken from each animal colon preserved in Carnoy's fixative. Each measurement was taken perpendicular to the upper and lower borders of the inner mucus layer, which are clearly delineated when this layer is well preserved. ImageJ software was used for data acquisition. For each time point, the mean absolute value from each mutant mouse was divided that of each WT mouse, and multiplied by 100 to get percent thickness relative to WT mice, and then an average percent thickness was obtained for each mutant mouse. The final values are the mean percent thickness of mutant vs. WT mice, which are assigned a value of "100%". A similar strategy was used to calculated distance of microbiota to mucosa, except the mean absolute distances were determined.

Antibiotic treatment

Mice were given filter sterilized (0.22 μm) tap water containing 1g/l each of metronidazole, neomycin sulfate, ampicillin and 0.5 g/l of vancomycin (Sigma)[10], and 0.1% sucrose. Control mice were given water with 0.1 % sucrose. After 3 – 4 weeks, mice were euthanized. For streptomycin treatment, mice were orally gavaged with 20 mg streptomycin in a volume of 100 μl sterile ddH_2O, once per day for 2 days, and then euthanized.

Bacterial enumeration

Total bacteria was enumerated by real-time qPCR for the gene encoding the highly conserved region of the 16 rRNA gene using the universal primers we have already optimized.[10] DNA was extracted from 100 mg of stool using the Qiagen Stool mini kit, as well as from the tissues using the Qiagen DNEasy Blood and Tissue Kit. SYBR-green based quantitative PCR was performed using primers described above.

Mucus isolation

Colons from WT and *O*-glycan deficient mice were opened up longitudinally, and stool contents were carefully removed. Adherent mucus was gently scraped off with a glass slide, using gentle pressure. Secretions were placed in a microtube along with 0.2 ml ice-cold PBS containing 2× complete protease inhibitors (Roche), and 5 volumes of guanidium chloride extraction buffer (6 M GuCl, 0.1 M Tris pH 8.0, 1 mM EDTA) was added. The secretions were dispersed with a Dounce homogenizer (3 strokes) and then extracted overnight at 4°C on a rotator. Following extraction, sample were reduced twice with 100 mM DTT, once for 5 h, and the other for overnight at 37°C to solubilize the gel-forming mucin. The mucus was then alkylated with 250 mM iodoacetamide on a rotator overnight at RT, in the dark. The reduced and alkylated mucin was dialyzed into ddH_2O, and the post-dialyzed sample was concentrated by centrifugation with an Amicon Centrifugal Filtration Unit, 100 kDa MWCO. The concentrated sample was then stored in −20°C until analyzed.[19]

Composite SDS agarose-polyacrylamide gel glectrophoresis (SDS AgPAGE)

Composite agarose-polyacrylamide gel is used to analyze large molecular weight glycoproteins.[45] This is made up of a gradient of 0.5–1.0% agarose, 0–10% glycerol, 0–6% acrylamide.[45] Mucins were electrophoresed for 4 h at 30 mA on ice, and the gels were processed for further analysis via periodic acid/Schiff (PAS) staining, using the Pierce Glycoprotein Staining Kit (ThermoScientific). Gels were imaged on an Epson scanner.

Mucus degradation assay

Semi-purified mucin was quantified by Dc Protein Assay (Biorad). 5 ug of WT and DKO mucin were treated with PBS or 0.01 to 1 mU pronase (Calbiochem) incubated for 30 min in 1 × PBS pH 7.0 at 37°C in a 30 μl volume. 6× sample buffer was then added and samples were boiled for 5 min to deactivate the pronase, then separated by AgPAGE and analyzed by in-gel staining with PAS and western blot.

Western blotting, densitometry, and membrane overlays

Mucin samples separated by AgPAGE were transferred onto a PVDF membrane via wet transfer at 100 V for 1.5 h on ice. The membrane was blocked with 5% milk in TBST (pH 7.6), and then incubated with polyclonal rabbit anti-Muc2-C3 antisera$_8$ (1:1000) overnight at 4 °C. Membranes were washed with TBS-T, incubated with HRP-conjugated goat anti-rabbit IgG for 1 h at RT, washed and detected with SuperSignal Enhanced Chemiluminescence reagent (Thermoscientific), and developed using film and/or a GeneSys Chemidoc (Syngene). For subsequent blotting for fucosylated glycans, membranes were stripped using 0.1% SDS, 0.2 M Glycine, 1% Tween 20, pH 2.2. and reblocked as above, as well with the Streptavidin/Biotin blocking kit (Vector labs) and probed with biotin-conjugated UEA1 (2 μg/ml) for 2 h at RT, washed, then incubated with HRP-conjugated Streptavidin (Jackson, 2 μg/ml) for 40 min, and detected and visualized as above. Densitometry was performed on inverted greyscale images using ImageJ software and analyzed using MS Excel and Prism (GraphPad) software. For membrane overlays, blot images of Muc2 and UEA1 (analyzed on the same blot) were opened in Adobe Photoshop CS3, inverted, false colored using the Adjustments→ Selective color option in the Image pull down menu, overlayed by adjusting the opacity of the top layer. Markers were used for precise alignments.

RNA and gDNA extraction and quantitative RT-PCR—Total RNA was extracted from flash frozen colon tissue using the RNeasy kit (Qiagen) and 1.5 μg was reverse transcribed using the Omniscript RT kit (Qiagen) according to the manufacturer's instructions. For bacterial 16S rRNA analysis, bacterial gDNA was extracted from mouse fecal pellets using the Stool mini Kit (Qiagen) and 5 ng was used for PCR. Quantitative PCR was performed using 2× iQ MasterMix and a CFX-96 system (Bio-Rad). Cytokine primer sequences are *tnf* Fwd: 5'-CATCTTCTCAAAATTCGAGTGACAA-3' Rev: 5'-TGGGAGTAGACAAGGTACAACCC-3'; *il6* Fwd: 5'-GAGGATACCACTCCCAACAGACC-3' Rev: 5'-AAGTGCATCATCGTTGTTCAT-3'; *il1beta* Fwd: 5'-CAGGATGAGGACATGAGCACC -3' Rev: CTCTGCAGACTCAAACTCCAC-3'; and 18S rRNA Fwd: 5'-GTAACCCGTTGAACCCCATT-3' Rev: 5'-CCATCCAATCGGTAGTAGCG-3'. Group-

specific primers for Bacteroidales order, *Lactobacillus sp*, *Bifidobacterium sp*, and *Clostridium sp*. were obtained from Wlodarska et al (2010),[46] and *Prevotella* sp. were obtained from Matsuki et al (2002).[47] Expression analysis was carried out using the Bio-Rad CFX manager 3.0 (using the $^{\Delta\Delta}$Ct method for relative normalized expression, and $^{\Delta}$Ct for relative expression). All relative normalized expression data used 18S rRNA mRNA as the internal control.

Statistics

Data was plotted and analyzed using GraphPad Prism V5.0. Error bars represent standard deviation (SD) unless otherwise indicated. All data sets passed the D'Agostino & Pearson omnibus K2 normality tests. Student's *t* test was used to analyze the difference between 2 groups. 1-way ANOVA followed by Bonferroni post-test was used to analyze the difference between 3 or more groups. A *P* value less than 0.05 was considered to be significant.

Supplementary Material

Refer to Web version on PubMed Central for supplementary material.

Acknowledgments

We would like to thank Dr. Courtney Griffin for technical support. This work was supported by NIH grants RR018758, R01DK085691, UL1TR000124, U01AI095473; Chinese National Natural Science Foundation grants 81470825, 8151001178, 31400692, and 81172299; Swedish Research Council, The Swedish Cancer Foundation, The Knut and Alice Wallenberg Foundation; and the Crohn's and Colitis Foundation of America Research Fellows Award 285148.

References

1. Ford AC, Moayyedi P, Hanauer SB. Ulcerative colitis. BMJ. 2013; 346
2. Strober W, Fuss I, Mannon P. The fundamental basis of inflammatory bowel disease. J Clin Invest. 2007; 117:514–521. [PubMed: 17332878]
3. Johansson ME, Sjovall H, Hansson GC. The gastrointestinal mucus system in health and disease. Nat Rev Gastroenterol Hepatol. 2013; 10:552–361.
4. Ley RE, Peterson DA, Gordon JI. Ecological and evolutionary forces shaping microbial diversity in the human intestine. Cell. 2006; 124:837–848. [PubMed: 16497592]
5. Pelaseyed T, et al. The mucus and mucins of the goblet cells and enterocytes provide the first defense line of the gastrointestinal tract and interact with the immune system. Immunol Rev. 2014; 260:8–20. [PubMed: 24942678]
6. Ambort D, et al. Calcium and pH-dependent packing and release of the gel-forming MUC2 mucin. Proc Natl Acad Sci U S A. 2012; 109:5645–5650. [PubMed: 22451922]
7. Johansson ME, Holmen Larsson JM, Hansson GC. The two mucus layers of colon are organized by the MUC2 mucin, whereas the outer layer is a legislator of host-microbial interactions. Proc Natl Acad Sci U S A. 2010; 108(Suppl 1):4659–4665. [PubMed: 20615996]
8. Johansson ME, et al. The inner of the two Muc2 mucin-dependent mucus layers in colon is devoid of bacteria. Proc Natl Acad Sci U S A. 2008; 105:15064–15069. [PubMed: 18806221]
9. Allen A, Hutton DA, Pearson JP. The MUC2 gene product: a human intestinal mucin. Int J Biochem Cell Biol. 1998; 30:797–801. [PubMed: 9722984]
10. Fu J, et al. Loss of intestinal core 1-derived O-glycans causes spontaneous colitis in mice. Journal of Clinical Investigation. 2011; 121(4):1657–1666. [PubMed: 21383503]

11. Larsson JMH, et al. Altered O-glycosylation profile of MUC2 mucin occurs in active ulcerative colitis and is associated with increased inflammation. Inflamm Bowel Dis. 2011; 17:2299–2307. [PubMed: 21290483]
12. Van der Sluis M, et al. Muc2-deficient mice spontaneously develop colitis, indicating that MUC2 is critical for colonic protection. Gastroenterology. 2006; 131:117–129. [PubMed: 16831596]
13. An G, et al. Increased susceptibility to colitis and colorectal tumors in mice lacking core 3-derived O-glycans. J Exp Med. 2007; 204:1417–1429. [PubMed: 17517967]
14. Brockhausen, I. Comprehensive Glycoscience. Kamerling, P., Editor-in-Chief: Johannis. , editor. Elsevier; 2007. p. 33-59.
15. Xia L, et al. Defective angiogenesis and fatal embryonic hemorrhage in mice lacking core 1-derived O-glycans. J Cell Biol. 2004; 164:451–459. [PubMed: 14745002]
16. Hang HC, Bertozzi CR. The chemistry and biology of mucin-type O-linked glycosylation. Bioorg Med Chem. 2005; 13:5021–5034. [PubMed: 16005634]
17. Robbe C, Capon C, Coddeville B, Michalski J-C. Structural diversity and specific distribution of O-glycans in normal human mucins along the intestinal tract. Biochem J. 2004; 384:307–316. [PubMed: 15361072]
18. Rakoff-Nahoum S, Paglino J, Eslami-Varzaneh F, Edberg S, Medzhitov R. Recognition of commensal microflora by toll-like receptors is required for intestinal homeostasis. Cell. 2004; 118:229–241. [PubMed: 15260992]
19. Png CW. Mucolytic bacteria with increased prevalence in IBD mucosa augment in vitro utilization of mucin by other bacteria. Am J Gastroenterol. 2010; 105:2420–2428. [PubMed: 20648002]
20. Norrsell H, Bengtsson J, Jovall PA, Hansson GC. N-linked glycopeptides with blood group determinants lacking neuraminic acid from the epithelial cells of rat small and large intestine. Eur J Biochem. 1992; 203:285–293. [PubMed: 1730235]
21. Barthel M, et al. Pretreatment of mice with streptomycin provides a Salmonella enterica serovar Typhimurium colitis model that allows analysis of both pathogen and host. Infect Immun. 2003; 71:2839–2858. [PubMed: 12704158]
22. Bergstrom KS, et al. Muc2 protects against lethal infectious colitis by disassociating pathogenic and commensal bacteria from the colonic mucosa. PLoS Pathog. 2010; 6:e1000902. [PubMed: 20485566]
23. Waksman SA. Streptomycin: background, isolation, properties, and utilization. Science. 1953; 118:259–266. [PubMed: 13089668]
24. Miller CP, Bohnhoff M. Changes in the Mouse's Enteric Microflora Associated with Enhanced Susceptibility to Salmonella Infection Following Streptomycin Treatment. J Infect Dis. 1963; 113:59–66. [PubMed: 14044094]
25. Rhodes JM, Gallimore R, Elias E, Allan RN, Kennedy JF. Faecal mucus degrading glycosidases in ulcerative colitis and Crohn's disease. Gut. 1985; 26:761–765. [PubMed: 2991089]
26. Dwarakanath AD, et al. Faecal mucinase activity assessed in inflammatory bowel disease using 14C threonine labelled mucin substrate. Gut. 1995; 37:58–62. [PubMed: 7672682]
27. Xu J, Gordon JI. Inaugural Article: Honor thy symbionts. Proc Natl Acad Sci U S A. 2003; 100:10452–10459. [PubMed: 12923294]
28. Wang Y, et al. Regional mucosa-associated microbiota determine physiological expression of TLR2 and TLR4 in murine colon. PLoS One. 2010; 5:e13607. [PubMed: 21042588]
29. Hu S, et al. Regional differences in colonic mucosa-associated microbiota determine the physiological expression of host heat shock proteins. Am J Physiol Gastrointest Liver Physiol. 2010; 299:G1266–G1275. [PubMed: 20864653]
30. Sonnenburg JL. Glycan foraging in vivo by an intestine-adapted bacterial symbiont. Science. 2005; 307:1955–1959. [PubMed: 15790854]
31. Martens EC, Roth R, Heuser JE, Gordon JI. Coordinate regulation of glycan degradation and polysaccharide capsule biosynthesis by a prominent human gut symbiont. J Biol Chem. 2009; 284:18445–18457. [PubMed: 19403529]
32. Martens EC, Chiang HC, Gordon JI. Mucosal glycan foraging enhances fitness and transmission of a saccharolytic human gut bacterial symbiont. Cell Host Microbe. 2008; 4:447–457. [PubMed: 18996345]

33. Zhang L, et al. O-glycosylation regulates polarized secretion by modulating Tango1 stability. Proc Natl Acad Sci U S A. 2014; 111:7296–7301. [PubMed: 24799692]
34. Perez-Munoz ME, et al. Discordance between changes in the gut microbiota and pathogenicity in a mouse model of spontaneous colitis. Gut Microbes. 2014; 5
35. Sommer F, et al. Altered mucus glycosylation in core 1 o-glycan-deficient mice affects microbiota composition and intestinal architecture. PLoS One. 2014; 9:e85254–e85254. [PubMed: 24416370]
36. Kashyap PC, et al. Genetically dictated change in host mucus carbohydrate landscape exerts a diet-dependent effect on the gut microbiota. Proc Natl Acad Sci U S A. 2013; 110:17059–17064. [PubMed: 24062455]
37. Rausch P, et al. Colonic mucosa-associated microbiota is influenced by an interaction of Crohn disease and FUT2 (Secretor) genotype. Proc Natl Acad Sci U S A. 2011; 108:19030–19035. [PubMed: 22068912]
38. McGovern DPB, et al. Fucosyltransferase 2 (FUT2) non-secretor status is associated with Crohn's disease. Hum Mol Gen. 2010; 19:3468–3476. [PubMed: 20570966]
39. Wenzel UA, et al. Spontaneous colitis in Muc2-deficient mice reflects clinical and cellular features of active ulcerative colitis. PLoS One. 2014; 9:e100217. [PubMed: 24945909]
40. Every AL, Chionh YT, Skene CD, McGuckin MA, Sutton P. Muc1 limits Helicobacter felis binding to gastric epithelial cells but does not limit colonization and gastric pathology following infection. Helicobacter. 2008; 13:489–493. [PubMed: 19166413]
41. McAuley JL, et al. MUC1 cell surface mucin is a critical element of the mucosal barrier to infection. J Clin Invest. 2007; 117:2313–2324. [PubMed: 17641781]
42. Rakoff-Nahoum S, Hao L, Medzhitov R. Role of toll-like receptors in spontaneous commensal-dependent colitis. Immunity. 2006; 25:319–329. [PubMed: 16879997]
43. Nenci A, et al. Epithelial NEMO links innate immunity to chronic intestinal inflammation. Nature. 2007; 446:557–561. [PubMed: 17361131]
44. Vijay-Kumar M, et al. Deletion of TLR5 results in spontaneous colitis in mice. J Clin Invest. 2007; 117:3909–3921. [PubMed: 18008007]
45. Johansson ME, Hansson GC. Analysis of assembly of secreted mucins. Methods Mol Biol. 2012; 842:109–121. [PubMed: 22259132]
46. Wlodarska M, et al. Antibiotic treatment alters the colonic mucus layer and predisposes the host to exacerbated Citrobacter rodentium-induced colitis. Infect Immun. 2011; 79:1536–1545. [PubMed: 21321077]
47. Matsuki T, et al. Development of 16S rRNA-gene-targeted group-specific primers for the detection and identification of predominant bacteria in human feces. Appl Environ Microbiol. 2002; 68:5445–5451. [PubMed: 12406736]

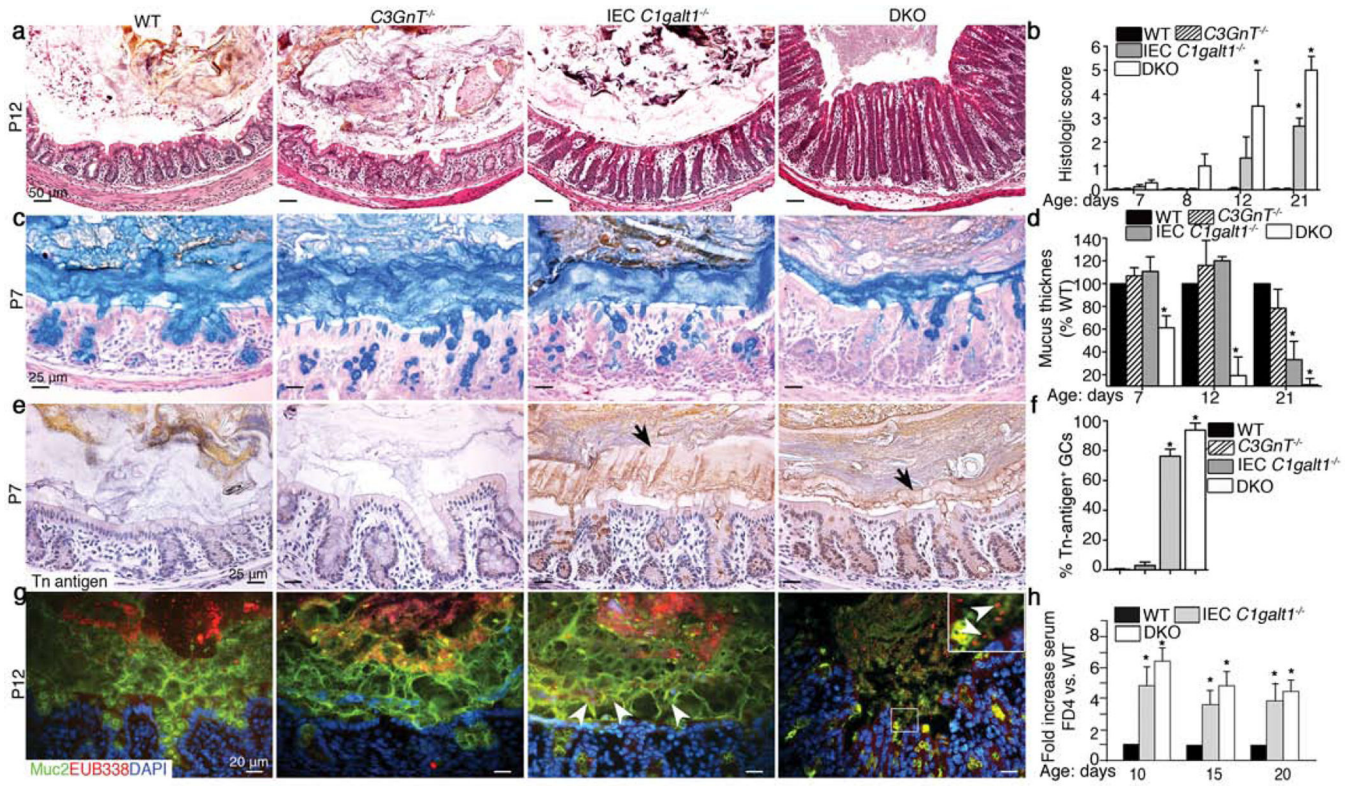

Figure 1. DKO mice have early onset and more severe colitis in the distal colon

(**a**) Representative images of H&E stained distal colons. P12 = postnatal day 12. (**b**) Histologic colitis score. (**c**) Representative AB staining of Carnoy's-fixed colonic sections. (**d**) Quantification of mucus thickness vs. WT mice. Error bars = SEM. (**e**) Representative images of Tn antigen immunohistochemistry (IHC) (brown) in colon sections. Arrow: top of mucus layer. (**f**) Quantification of Tn^+ cells from mice in (e). (**g**) Representative dual staining for Muc2 (IF, green) and bacteria (FISH, red), the latter using the universal EUB338 probe, on Carnoy's-fixed colonic sections. Inset, magnified image of boxed region. Arrowheads, bacteria. (**h**) Quantitation of serum FITC-Dextran, 4 kDa (FD4) 4 h after oral administration. Bars show average fold changes relative to WT mice. Data are representative of >2 independent studies with n = 4 – 6 mice/group. For (b), (d), and (h) *P < 0.05 vs. WT.

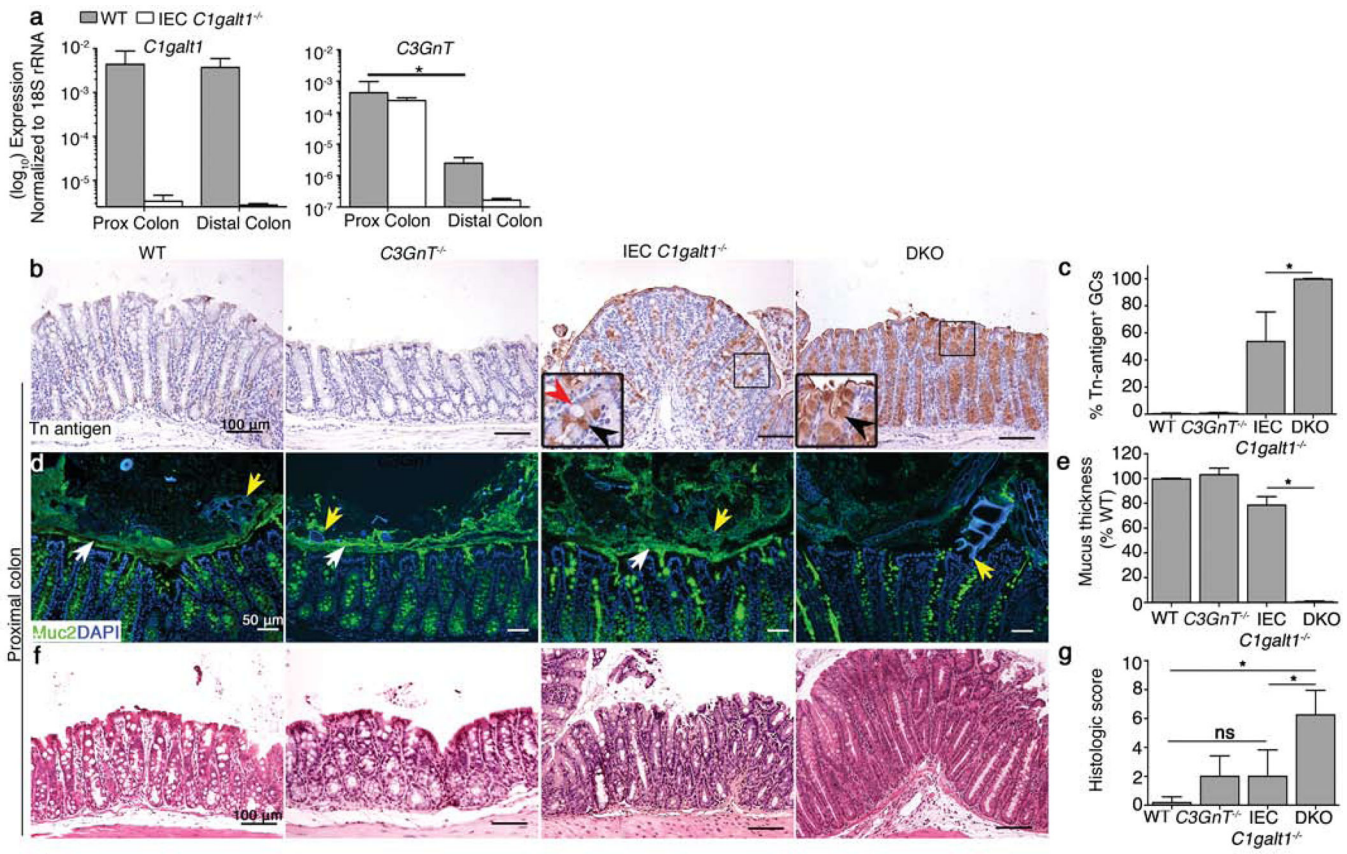

Figure 2. DKO mice exhibit defective mucus and spontaneous colitis in the proximal colon

(**a**) Gene expression analysis of enriched colonic crypt cells by RT-qPCR. (**b**) Representative IHC for Tn antigen (brown). Inset, magnified image of boxed regions. Arrowheads: red, Tn^{-} goblet cell; black, Tn^{+} goblet cell. (**c**) Quantification Tn^{+} goblet cells. Error bars = SEM. (**d**) Representative IF staining for Muc2 on Carnoy's-fixed sections. Arrows: White, mucus layer; yellow, luminal food particle. (**e**) Quantification of mucus thickness vs. WT mice. (**f**) Representative H&E staining of proximal colonic sections. (**g**) Histologic colitis score. Data are representative of 2 independent studies, n = 4 – 6/group; WT mice are littermate controls. *P < 0.05, student's *t* test for (a), (c), (e) and 1 way ANOVA with Bonferonni post-test for (g).

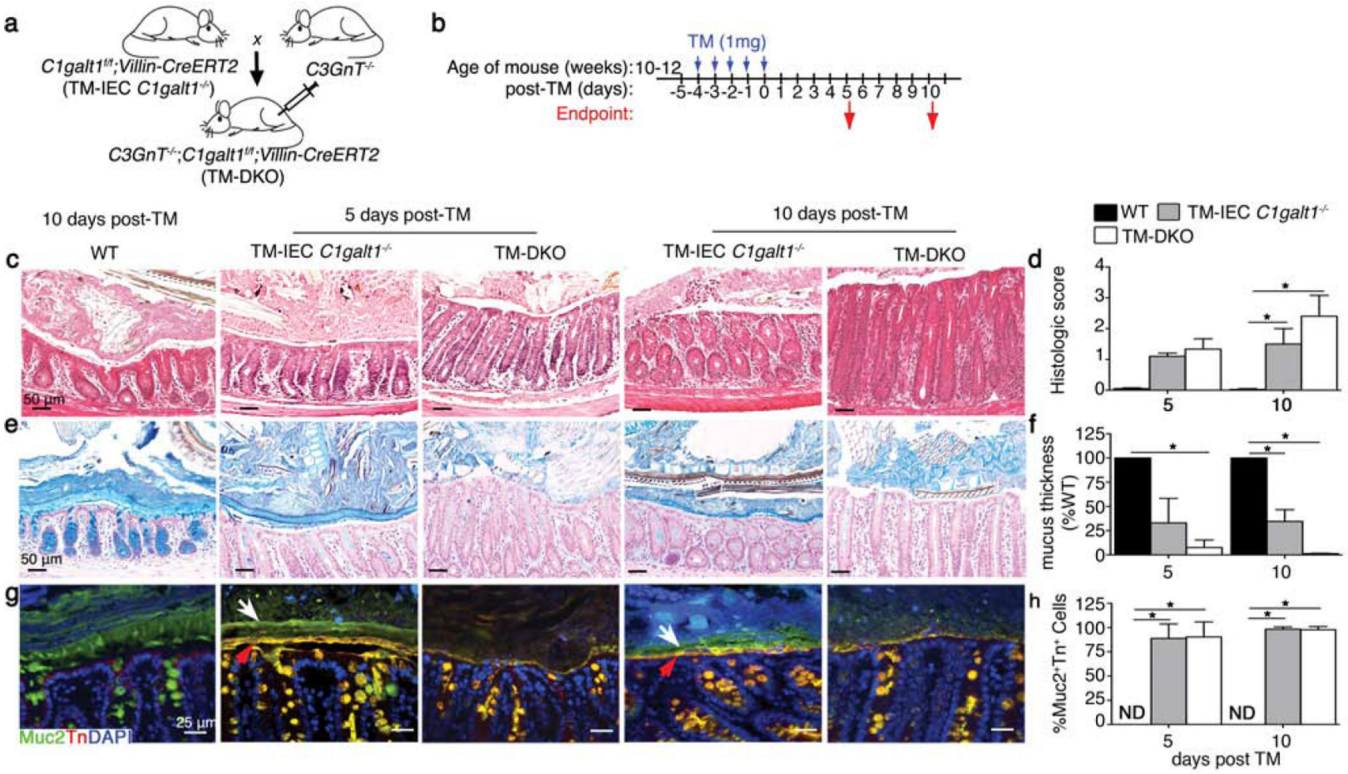

Figure 3. Deficiency of core 1- and 3-derived *O*-glycans impairs mucus layer and causes colitis in adult mice

(**a**) Generation of inducible DKO mice. (**b**) Experimental design. (**c**) H&E staining of carnoy's fixed distal colon sections. (**d**) Histologic colitis score. (**e**) Representative AB staining on Carnoy's fixed colon sections. (**f**) Quantification of mucus thickness vs. WT mice (from Muc2 stain). (**g**) Dual IF for Muc2 (green) and Tn antigen (red); dual $Muc2^{+}Tn^{+}$ cells are yellow (white arrow). Arrowheads: white, Tn^{-} portion of mucus; red, Tn^{+} portion of mucus. (**h**) Quantification of dual $Muc2^{+}Tn^{+}$ cells. For all bar graphs, error bars = SEM. Results are representative of 2 independent experiments, n = 4 – 6 mice/group/time point. TM-treated WT littermates are experimental controls. *P < 0.05 vs. TM-treated WT mice, 1 way ANOVA with Bonferroni post test.

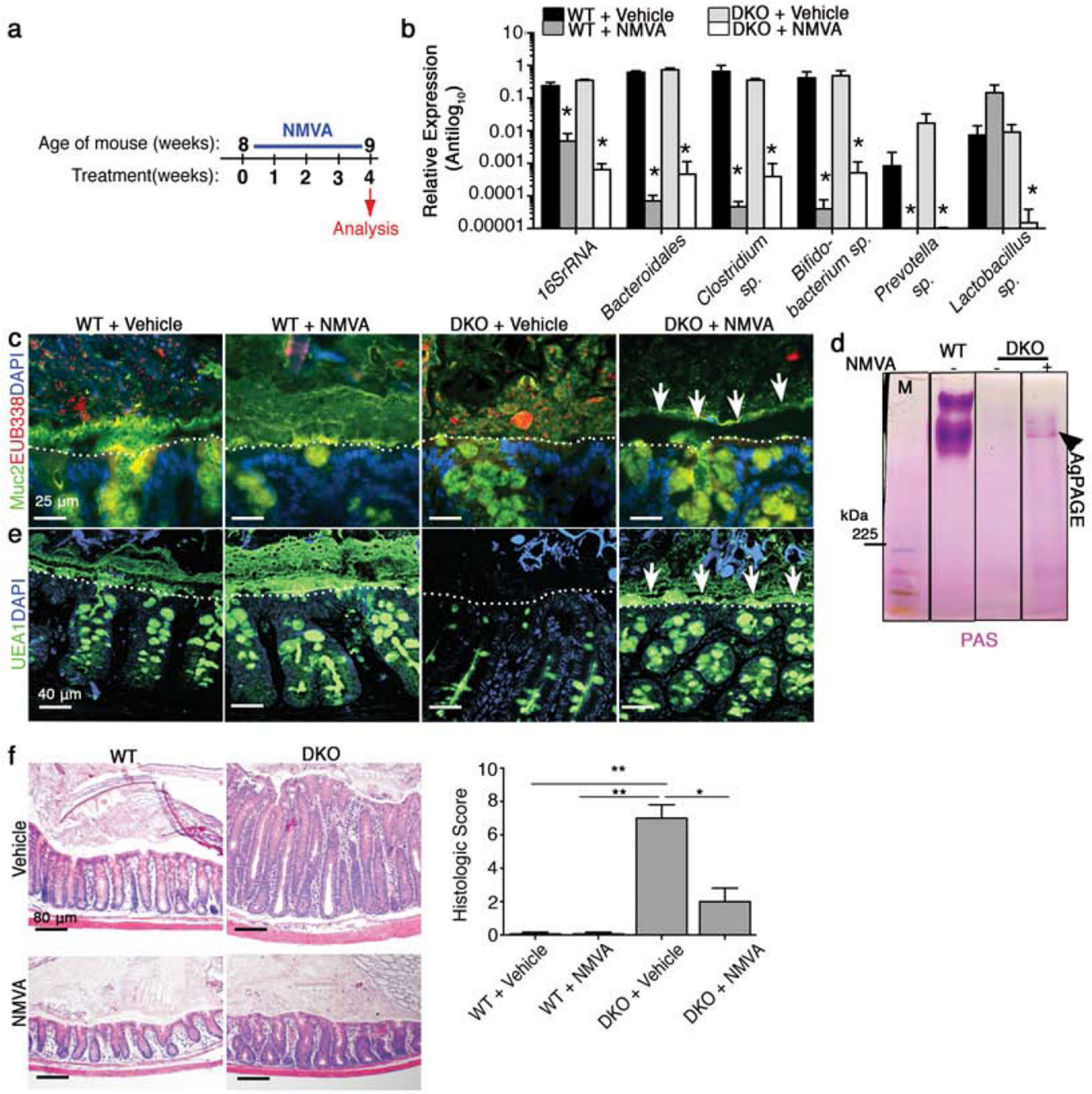

Figure 4. Microbial depletion rescues defective mucus layer function and ameliorates colitis in DKO mice

(**a**) Experimental design. (**b**) qPCR of bacterial universal and group-specific 16S RNA gene from fecal gDNA.. (**c**) Representative dual Muc2/EUB33 staining. Arrow, mucus layer. (**d**) Composite AgPAGE analysis of semipurified murine colonic mucin, visualized by PAS staining (magenta). Arrow, mucin band in DKO. (**e**) IF staining for the lectin UEA-1. Arrow, mucus layer. (**f**) Representative H&E staining of distal colon sections. *Right:* histologic damage score. Results are representative of 2 independent experiments, n = 4 mice/group.

WT mice are experimental controls. *P < 0.05 and **P < 0.01 vs. vehicle-treated WT, 1 way ANOVA with Bonferroni post-test.

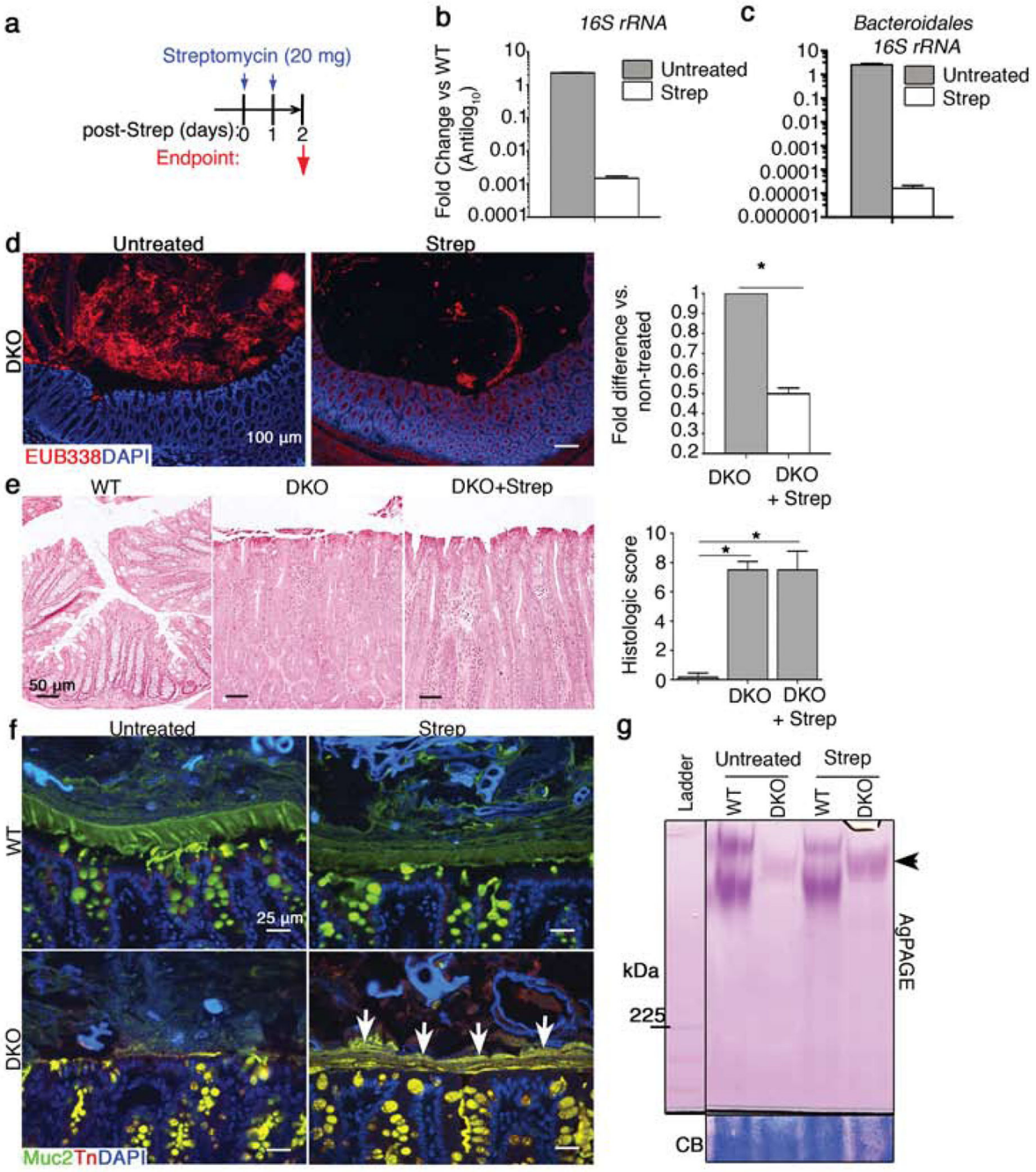

Figure 5. Loss of the mucus barrier in DKO deficient mice is dependent upon the microbiota but not inflammation

(**a**) Experimental design for short-term microbial depletion. (**b**) qPCR of total bacterial universal 16S RNA gene. (**c**) qPCR of bacterial 16S RNA gene specific for Bacteroidales order. (**d**) Representative FISH using EUB338 to stain bacteria (red). Right: Relative quantification of FISH signal in lumen. (**e**) Representative H&E of distal colon tissues. *Right;* histologic damage score. (**f**) Dual IF for Muc2 (green) and Tn antigen (red) on Carnoy's-fixed colonic sections. Arrows, dual $Muc2^{+}Tn^{+}$ mucus layer. (**g**) Composite

AgPAGE analysis of semipurified murine colonic mucin, visualized by PAS staining (magenta). Arrow, DKO Muc2 mucin band. CB, Coomassie Blue loading control. Results are representative of 3 independent experiments, 3 – 6 mice/group. Non-treated WT or DKO are experimental controls. *$P < 0.05$, student's *t* test.

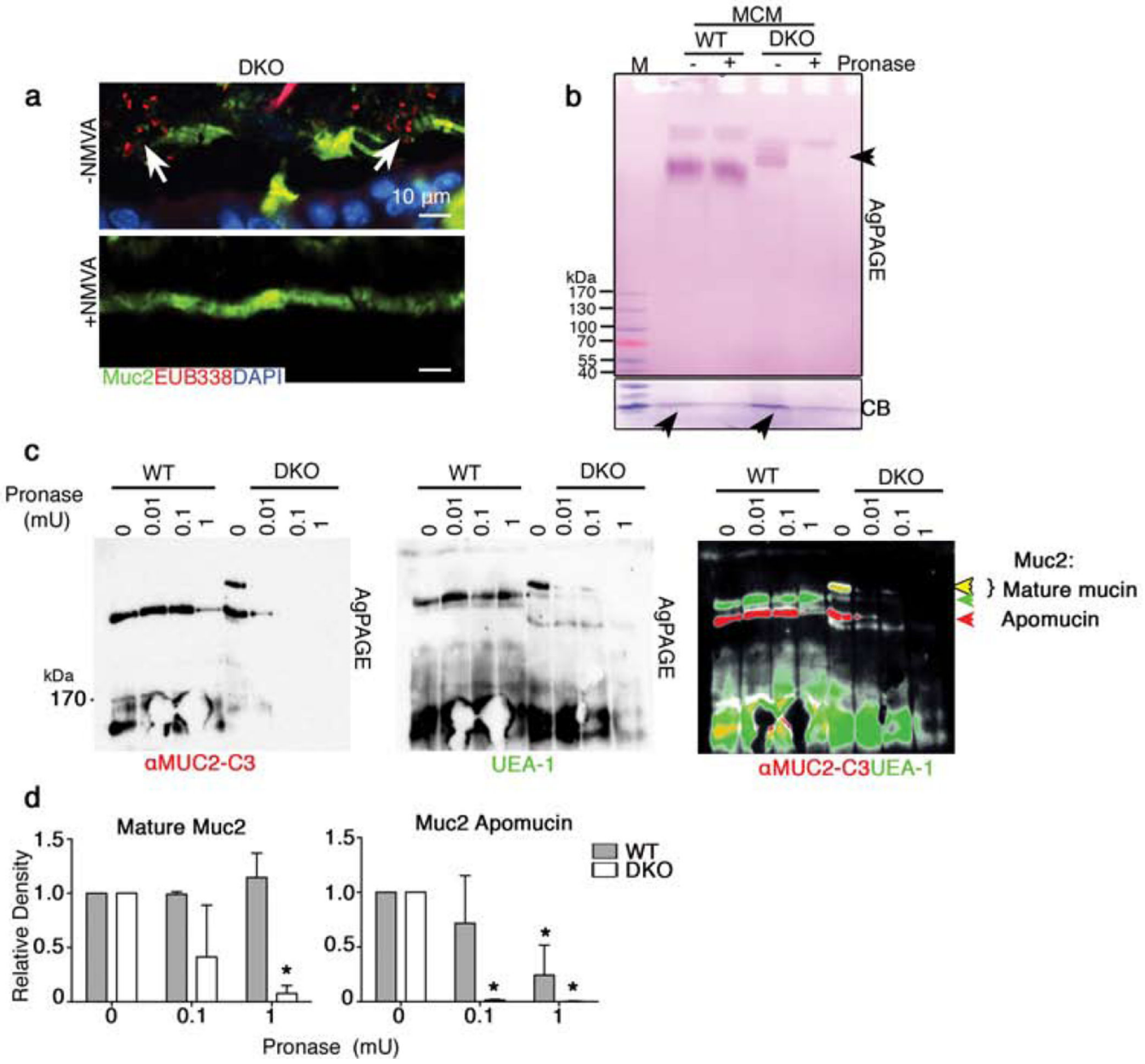

Figure 6. *O*-glycans protect Muc2 from bacterial protease-mediated degradation

(**a**) Dual Muc2/FISH staining. Note: images are from mice on a gel-food diet, which allowed preservation of broken mucus in untreated DKO mice. Arrows, bacteria. (**b**) PAS-stained composite AgPAGE gel of mucin derived from streptomycin-treated mice. CB, Coomassie Blue loading control. (**c**) Western blot for Muc2 protein (αMuc2-C3) and Fucosylated Muc2 (UEA1). (**d**) Densitometry of mature and immature Muc2 bands in WT and DKO mice. Error bars, SEM. Degradation studies are representative of 3 separate experiments, the third with independently derived mucin samples. *P < 0.05 vs. 0 mU, student's *t* test.